

Modeling and Characterization of a Fiber Optic Information Transmission System in the City Of Kinshasa.

Mumay Muluba¹, LidingaMobonda Flory², MeniBabakidi Narcisse³,
DondoMebukila François⁴, CimbelaKasongo Joseph.G⁵, PasiBengiMasata
André⁶.

Abstract: In this article, we model and characterize the physical parameters of the information transmission network using fiber optic technology in the city of Kinshasa. The various mathematical models make it possible to determine the optical fibers have, in the spectral window generally used, a very important usable band (approximately 15 THz around the wavelength 1.55 μm). Theoretically, the data rates that can be transmitted are therefore extremely high.

This article is to model and characterize the number and size of information exchanged which are increasingly important. Nevertheless, the electronic processing of electrical signals before modulation and after detection does not reach such frequencies. This is why various solutions have been devised to take advantage of the capacities of fiber optics and therefore increase the transfer of information on the same channel. In most cases, the principle remains the same: use N signals at bit rate D equivalent in terms of capacity to a signal at bit rate $N*D$, which is currently unfeasible. This is called multiplexing, and the data rates transported would now be higher. The concentrated signal of the streams of various origins is called a multiplex signal. To preserve the integrity of each signal on the channel, multiplexing introduces, between the signals, a temporal, spatial or frequency separation. These phenomena being physical, we will model them and simulate their results, finally, to analyze their impact in an optical fiber information transmission link.

Key words: Modeling, Characterization, Transmission system, Information, Fiber optics.

Date of Submission: 06-03-2023

Date of acceptance: 19-03-2023

II. OPERATING PRINCIPLE

II.1 Parameter equations

II.1.1 Optical power

The optical power delivered by one face of a laser diode is expressed by the relationship:

$$P_{opt}(I) = \eta_d \left(\frac{h\nu}{2e} \right) (I - I_{th}) \quad (2.1)$$

The role of the optical cavity is to make it possible to obtain the useful gain allowing the emission of photons, to facilitate the selectivity in frequency or in wavelength.

II.1.2 Wave length

The diffraction grating, also used to make integrated filters, ensures wavelength selectivity by increasing the losses of the cavity except at the desired frequency (figure 2.3).

The relation allowing to have the desired wavelength λ_m is:

$$\lambda_m = \frac{\lambda_0}{n} = \frac{2a}{m} \quad (2.2)$$

II.1.3 Noise in lasers

Like any oscillator, a semiconductor laser generating an optical signal is not ideal; its emission spectrum has amplitude noise and frequency noise. This noise constitutes one of the limitations in the operation of any optical communications system, since it brings constraints on the detection of the signal at the level of the receiver.

This noise originates in the spontaneous emission process within the laser diode, mainly due to optical phase and frequency fluctuations. It is characterized by the RIN (relative intensity noise) which is expressed by the relationship:

$$RIN(f) = \frac{(\Delta P_{opt})^2}{(P_{opt})^2} \quad (2.3)$$

$(\Delta P_{opt})^2$: represents the square of the optical and optical power fluctuations $(P_{opt})^2$, the square of the average laser emission optical power.

This ratio is often expressed dB/Hz using the following relationship:

$$RIN(f) = 10 \log RIN(f) \quad (2.4)$$

II.1.4 Electrical noise power N_E

The power is measured with the spectrum analyzer resulting from three contributions, the noise of the laser N_L ; the shot noise N_q of the photodiode which is directly linked to the optical power detected, and therefore to the photocurrent; the thermal noise N_{th} of the measurement chain, determined when the laser is off.

Either:

$$N_E = N_L + N_q + N_{th} \quad (2.5)$$

The measurement of the power emitted by the laser and the determination of N_L then make it possible to deduce the value of the RIN therefrom.

II.1.5 Wave phase shift

When an electric field E is applied, this results in a modification of the refractive index of the material of the optical guide, which has the consequence of varying the phase of the guided wave and of generating a variable delay of the optical wave. Over a propagation distance of length L , the output light wave is phase shifted with respect to the incident wave, this phase shift being given by the relationship:

$$\Delta\varphi = 2\pi L \cdot \frac{\Delta n}{\lambda} \quad (2.6)$$

With :

$$\Delta n = n^3 \dot{r} \frac{E}{2} \quad (2.7)$$

When the field is applied longitudinally, the voltage causing a phase shift of π is deduced:

$$V_{\lambda/2} = \frac{\lambda}{n^3 \dot{r}} \quad (2.8)$$

Since :

$$V = ExL \quad (2.9)$$

This so-called "half-wave" voltage is characteristic of the electro-optical material.

II.1.6 Photo-detector

A photo-detector is characterized by its absorption coefficient: it depends on the material used and characterizes the penetration of light inside the semiconductor. It is measured in cm^{-1} . Its quantum efficiency η : it represents the ratio of the number of photo-created carrier pairs to the number of incident photons. Its value is generally less than 1 and increases with the thickness of the absorbent zone; it is between 0.5 and 0.8. It is defined by the following relation:

$$\lambda = \frac{I_{ph}/e}{I_{ept}/h\nu} \quad (2.10)$$

If we include the other possible losses due to the imperfections of the material (traps, dislocations), we characterize the material by its external quantum efficiency $e\lambda$ which is slightly lower. Sensitivity S : it defines the ratio of the photo-current detected to the luminous flux (or to the optical power received), and is expressed in (A/W):

$$S(\lambda) = \frac{I_{ph}}{P_{opt}} = \eta \frac{e\lambda}{h \cdot c} \quad (2.11)$$

II.1.7 Johnson noise or thermal noise

Thermal noise, or Johnson, represents the random fluctuations of carriers inside a resistor as a result of thermal agitation. The thermal noise current spectral density linked to the load resistance of the photodiode is represented by the relationship:

$$(i_{th}^2) = \frac{4kT}{R} \quad (2.12)$$

II.1.8 Shot noise

It is related to the passage of carriers in the potential barrier. Its current spectral density is given by:

$$(i_n^2) = 2e I_{ph} \quad (2.13)$$

II.1.9 Dark current noise

Fluctuations in the dark current contribute to noise by the relationship:

$$(i_{obs}^2) = 2e I_{obs} \quad (2.14)$$

III.2 Nonlinear Equivalent Electrical Intrinsic Model

The absorption of incident light in an electro-absorption modulator varies greatly depending on the voltage V_M applied to the modulator: the modulator is transparent for a zero voltage and absorbent for a negative voltage. This property is characterized by the static extinction ratio $SER(V_M)$ (static extinction ratio) of the modulator, defined as the ratio between the optical powers at the output P_{out} of the MEA for a non-zero and zero electrical bias voltage V_M respectively:

$$SER(V_M)_{dB} = \frac{P_{out}(V_M)}{P_{out}(V_M = 0V)} \quad (2.15)$$

Or in decibels:

$$SER(V_M)_{dB} = 10 \times \log SER(V_M) \quad (2.16)$$

II.1.11 Specific rational function FNL(V_M)

In order to be able to be integrated directly into ADS, the measured curve of the $SER(V_M)$ was modeled by a specific rational function $FNL(V_M)$ of the form:

$$F_{NL}(V_M) = \frac{A_0 + \sum_{k=1}^6 A_k x V_M^k}{1 + \sum_{k=1}^4 B_k x V_M^k} \quad (2.17)$$

In this equation, the value of the constants A_k ($k=0$ to 6) and B_k ($k=1$ to 4) are obtained by interpolation, using for example the Matlab software.

III Simulation of results and interpretation

III.1 Simulation of results

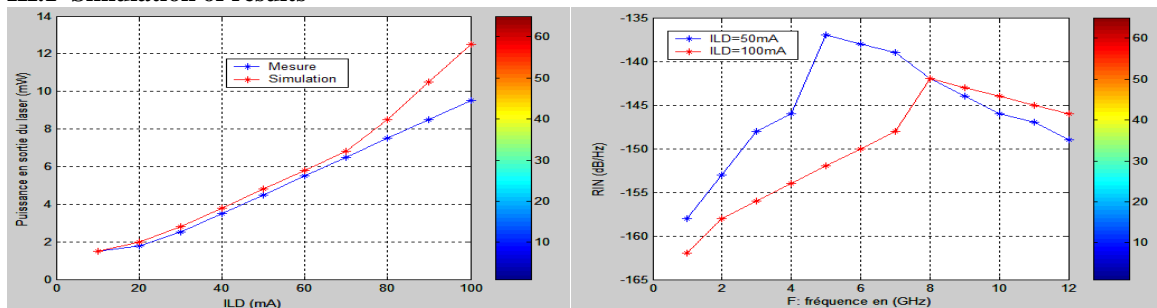


Figure 3.1: Measured and simulated static P-I responses of the DFB laser Figure 3.2: Measured and simulated RIN curves of the DFB laser

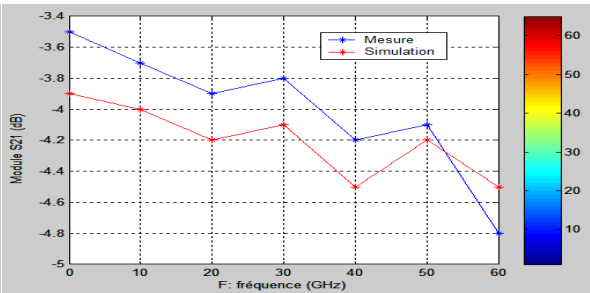
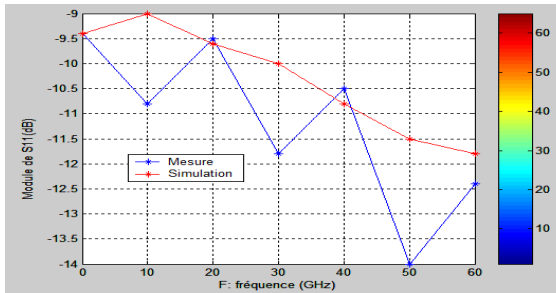


Figure 3.3: MEA access line input adaptation Figure 3.4: MEA Access Line Insertion Losses

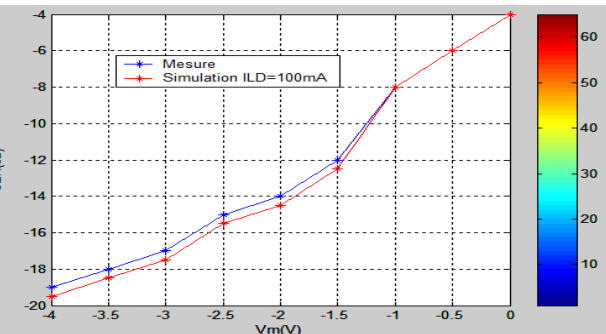
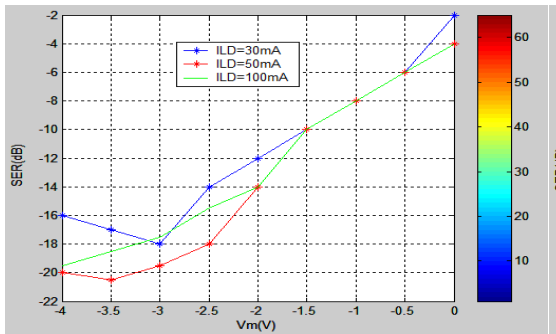


Figure 3.5: Extinction rate of 75 μm MEA Figure 3.6 : Comparison of measured and simulated SER (VM) for ILD=100 mA

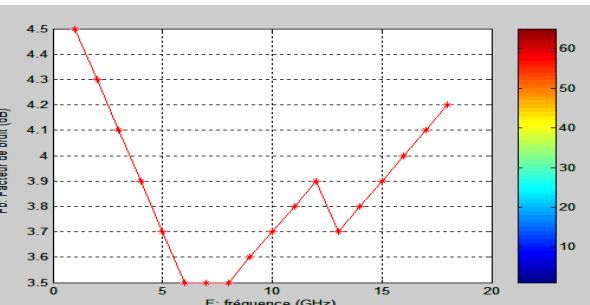
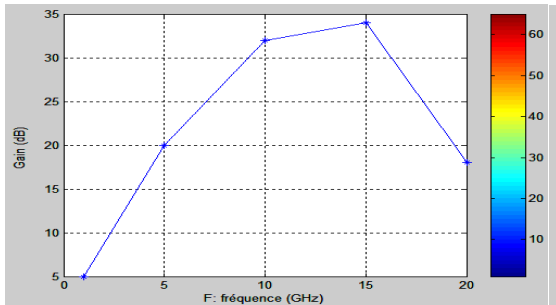


Figure 3.7: LNA gain as a function of frequency Figure 3.8 :LNA noise figure as a function of frequency

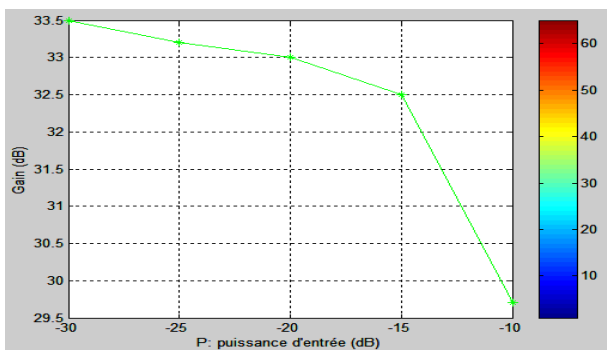


Figure 3.9 :LNA compression point measurement at 4 GHz

III.2 Interpretations

The equivalent circuit diagram of the DFB laser is based on the one hand on the two continuity equations of electrons and photons and on the other hand on an analogy between an electric current and an optical power. Noise sources modeled by Langevin forces represent random variations in the number of electrons and photons due to spontaneous emission. The RIN (Relative Noise Intensity) noise and the non-linearity of the laser output power are also taken into account in the laser model.

The electrical parameters of the model are determined from certain physical quantities of the laser and measurements such as the static power-current characteristic (P-I) and the RIN.

The simulated RIN noise and static responses are shown in Figures 2.18 and 2.19. The laser has a threshold current of 9 mA, a sensitivity of 0.18 W/A and an optical wavelength of 1535 nm. A good agreement of the simulation results with the measurements of the power-current curve and of the noise RIN as a function of frequency makes it possible to validate the electrical model of the laser both in static and dynamic conditions. However, the saturation of the laser could not be modeled.

IV. CONCLUSION

We have seen that this article consisted in modeling and characterizing The model of the low noise amplifier (LNA) was developed on the one hand from the measurements of its parameters S and of its noise factor as a function of the frequency and d other than from the determination of its compression point at the frequency of 4 GHz, corresponding to the selected OFDM frequency.

The S parameters were measured using an HP 8720D vector network analyzer calibrated in reflection and transmission between 0.05 and 20.05 GHz. Similarly, the 1 dB compression point was determined on the analyzer by performing a power sweep between -30 dBm and -10 dBm at 4 GHz.

Noise measurements were made between 1 and 18 GHz using a spectrum analyzer from Agilent Technologies (E4446A), equipped with the noise option (option 110). In order not to have too long simulation times, we used under ADS a predefined RF component (Amplifier) which is in fact a black box in which the measured characteristics of the LNA are defined, namely, its gain, its factor of noise and its compression point at a given frequency.

At the frequency of 4 GHz, and for a bias of 12 V-160 mA, the LNA has a gain of 32.9dB, a noise figure of 3.8 dB and an output power at the compression point of 14.8 dBm, which is in accordance with the manufacturer's data.

We have described the principle of operation and the main characteristics of the components involved in a mixed opto-microwave link used in radio systems on fiber. In addition, the electrical models associated with each of the components involved. The models of the DFB laser, the optical fiber and the photodiode used and which has a strong experience in the field of optoelectronic components. These models were then optimized from the results of measurements obtained on each of them.

REFERENCES

- [1]. LE BRUN Christine, "COMSIS: Modeling of component and application to the simulation of optical communication systems", Applied Optics, September 1998, Vol. 37, n°26, pp. 6059-6065.
- [2]. RICE S.O., "Envelops of narrow-band signals", Proc. of the IEEE, July 1982, Vol. 70, n° 7.
- [3]. PICINBONO B. et MARTIN W., "Représentation des signaux par amplitude et phase instantanées", Annales des Télécommunications, Mai-Juin 1983, Vol. 38, n° 5 et 6.
- [4]. HELMS H.D., "Fast Fourier transform method of computing difference equations and simulating filters", IEEE Transactions on Audio Electroacoustic, 1967, Vol. AU-15, pp. 85-90.
- [5]. ALLEN J.B., "Fastfilt : an FFT based filtering program", Programs for Digital Signal Processing, IEEE Press, 1979, Sec. 3.1, pp. 1-5.
- [6]. JOINDOT Irène et Michel, Les Télécommunications par fibres optiques, Collection Technique et Scientifique des Télécommunications, Paris : Dunod et CENT-ENST, 1996.

BIOGRAPHY

MUMAY MULUBA Jean, Master recherche en 2012 ESP-University Cheikh Anta Diop Dakar. Doctor student of University national pedagogy of Kinshasa-Congo. of Applied Sciences



Pof.Dr.Ir Lidinga Mobonda Flory, PhD In Engineering Sciences.Of Electricity.
ENSP-UMNG Electrical Engineering Research Laboratory
Teacher-Researcher at ISTA-Boma





Prof. Dr. Ir Narcisse MeniBabakidi, Ph.D. University Michoacana of San Nicolas of Hidalgo (UMSNH) Mexico .2017-2021, Teacher-Researcher at ISTA-Kinshasa



Dodo Mebukila Francois
Assistant teacher at ISTA-Boma. Master Student in engineering sciences, the computer network engineer.



Prof. Dr Cimbela Kasongo Is an physic, he received, from the University National Pedagogy of Kinshasa-Congo. He is presently lecturer at the University National Pedagogy of Kinshasa-Congo. Dept.



Pof. Dr. Ir Pasi Bengi Masata, PhD en Sciences Appliquées. Enseignant-Chercuer à l'ISTA-Kinshasa